Click Here for Full Article

Stratospheric influence on the tropospheric circulation revealed by idealized ensemble forecasts

E. P. Gerber,[1] C. Orbe,[2] and L. M. Polvani[2]

[1]   The coupling between the stratosphere and troposphere following Stratospheric Sudden Warming (SSW) events is investigated in an idealized atmospheric General Circulation Model, with focus on the influence of stratospheric memory on the troposphere. Ensemble forecasts are performed to confirm the role of the stratosphere in the observed equatorward shift of the tropospheric midlatitude jet following an SSW. It is demonstrated that the tropospheric response to the weakening of the lower stratospheric vortex is robust, but weak in amplitude and thus easily masked by tropospheric variability. The amplitude of the response in the troposphere is crucially sensitive to the depth of the SSW. The persistence of the response in the troposphere is attributed to both the increased predictability of the stratosphere following an SSW, and the dynamical coupling between the tropospheric jet and lower stratosphere. These results suggest value in resolving the stratosphere and assimilating upper atmospheric data in forecast models. **Citation:** Gerber, E. P., C. Orbe, and L. M. Polvani (2009), Stratospheric influence on the tropospheric circulation revealed by idealized ensemble forecasts, *Geophys. Res. Lett.*, *36*, L24801, doi:10.1029/2009GL040913.

1. Introduction

[2]   The goal of this study is to investigate the coupling between the stratosphere and troposphere following a Stratospheric Sudden Warming (SSW). By computing the Northern Annular Mode (NAM) index on each pressure level independently, *Baldwin and Dunkerton* [2001] found that SSWs tend to precede an equatorward shift of the tropospheric midlatitude jet by roughly 10 days, and that the tropospheric anomalies, on average, persist for two months. This coupling, however, is not entirely robust: some stratospheric events "reach" the troposphere, but others produce little effect [*Baldwin and Dunkerton*, 2001, Figure 1]. In addition, while the negative signal in the NAM appears to propagate downward from the stratosphere, the direction of causality may not be so obvious; *Plumb and Semeniuk* [2003] have shown in a stratosphere-only model that similar, seemingly downward propagating signals can be driven exclusively by the lower boundary. As SSW events are initiated by increased planetary wave fluxes from the troposphere [*Polvani and Waugh*, 2004], it is possible that the dynamics driving the NAM response might also be internal to the troposphere. This begs the question whether the stratospheric signal is more of a distraction, that is, a passive player in a cycle entirely driven by tropospheric dynamics. To discount this possibility, we perform a series of ensemble forecast experiments with an idealized General Circulation Model (GCM) to demonstrate the stratosphere's active role in maintaining the equatorward shift of the tropospheric jet.

[3]   Many earlier studies have probed stratosphere-troposphere coupling by perturbing the stratosphere, and observing the resulting impact on the troposphere [e.g., *Boville*, 1984; *Polvani and Kushner*, 2002; *Norton*, 2003; *Charlton et al.*, 2004; *Scaife et al.*, 2005]. Here we apply a different approach, instead perturbing the troposphere around SSW events to average away tropospheric internal variability, and so passively reveal the influence of the stratosphere. Our strategy exploits the difference in time scales between the troposphere and the stratosphere [*Baldwin et al.*, 2003]. We launch a large ensemble forecast before an SSW. Synoptic dynamics lead to rapid separation of ensemble members in the troposphere, erasing any tropospheric memory. Provided the same SSW occurs in each ensemble member, however, the stratosphere follows a more predictable trajectory due to the slow recovery time scales of the lower stratosphere. This allows us to isolate a robust signal in the troposphere as a direct response to stratospheric anomalies above.

[4]   Recent studies have explored the impact of the stratosphere on tropospheric predictability in ensemble forecasts. Case studies with an operational forecast model show increased predictability in both the stratosphere and the troposphere around the time of SSWs [*Kuroda*, 2008; *Mukougawa et al.*, 2009]. *Marshall et al.* [2009] find enhanced predictability in hindcasts where stratospheric initial conditions are included. Here we use an idealized GCM that captures stratosphere-troposphere coupling with fidelity [*Gerber and Polvani*, 2009], but with a computational efficiency that permits us to explore multiple warming events with large ensembles. The model is idealized only in its forcing, integrating the global primitive equations with horizontal and vertical resolutions comparable to that of comprehensive GCMs.

2. Methods

[5]   The atmospheric GCM used in this study integrates the dry primitive equations at T42 spectral resolution with 40 vertical levels extending to 0.7 Pa. It is run with perpetual January conditions, maintained by Newtonian relaxation to a prescribed temperature equilibrium profile and Rayleigh drag at the surface and upper boundary that approximate surface friction and gravity wave drag, respectively, as described in detail by *Polvani and Kushner* [2002]. The model is forced with a simple zonal wave-number 2 topography of maximum amplitude 3000 m, and

[1]Center for Atmosphere Ocean Science, Courant Institute, New York University, New York, New York, USA.
[2]Department of Applied Physics and Applied Mathematics and Department of Earth and Environmental Science, Columbia University, New York, New York, USA.
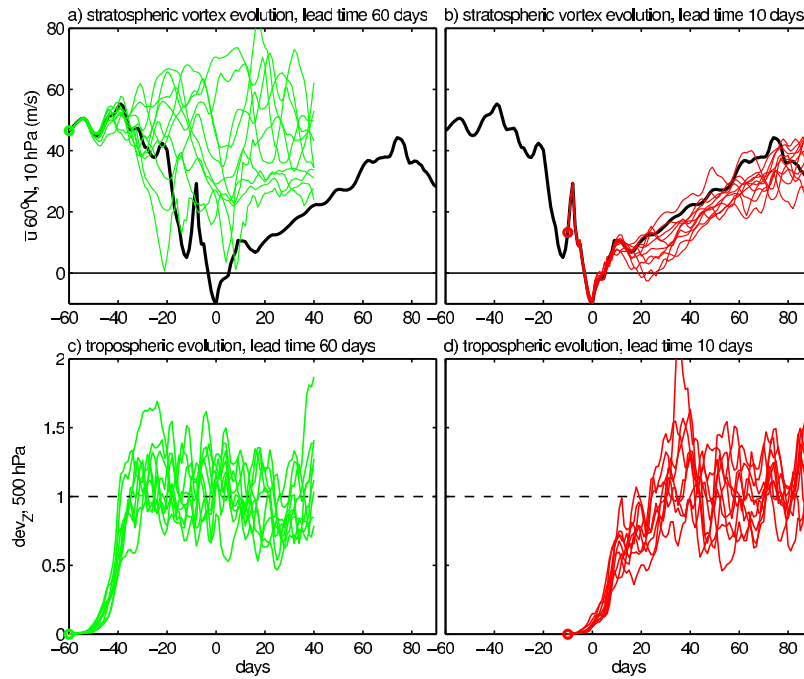
Figure 1. The ensemble forecast strategy, illustrated for SSW event 1. (top) the strength of the stratospheric vortex is quantified by the winds at 60°N and 10 hPa. The control is marked by the black curve, and ensemble members launched (a and c) 60 days and (b and d) 10 days before the event are marked by green and red curves, respectively. (bottom) The spread of ensemble trajectories away from the control in the troposphere is quantified by the normalized mean square deviation, dev_Z, at 500 hPa for the same two forecast experiments. Note the similarity in tropospheric spread in the two ensembles, in contrast to the difference in spread in the stratosphere.

the polar stratospheric vortex temperature is relaxed to a profile with lapse rate $\gamma = 4$ K/km to produce realistic stratospheric coupling on intraseasonal time scales. This is the configuration analyzed by *Gerber and Polvani* [2009], and further details can be found therein.

[6] A control integration of 10,000 days was run to produce a number of SSWs, identified with the standard WMO criterion, i.e., the zonal mean zonal wind at 60°N and 10 hPa reverses sign. From this integration, 4 events were selected with the intent to explore the impact of differences in the initial tropospheric state (positive vs. negative NAM) and depth of the warming. Around each of these events, 100 ensemble forecasts were created by adding small, random perturbations to wavenumbers 4–10 of the vorticity field in the Northern Hemisphere midlatitudes. The perturbations decay away from the surface as $a_p \exp[(p - p_s)^2/250^2]$, where pressure p is measured in hPa and p_s is the surface pressure, and so are almost entirely confined to the troposphere. The constant $a_p = 10^{-5}$ s^{-1} sets the root mean square amplitude of the perturbation at the surface.

[7] The NAM at each pressure level is the first EOF of the daily zonal mean zonal wind, weighted by the square root cosine of latitude. The NAM index is the area weighted projection of the daily mean wind anomalies onto the EOF, and normalized to have unit variance. The spread of the ensemble away from the control integration is quantified at each pressure level by the normalized mean square deviation,

$$dev_Z(p, t) = \frac{k_p}{2\pi^2} \int_o^{2\pi} \int_0^{\pi/2} (Z_{ensb}(\lambda, \phi, p, t) - Z_{ctrl}(\lambda, \phi, p, t))^2 \\ \cdot \cos\phi \ d\phi d\lambda, \quad (1)$$

here illustrated for the geopotential height Z. The subscripts 'ensb' and 'ctrl' refer to the ensemble member and control integrations, respectively, and λ and ϕ are longitude and latitude. The deviation $dev_Z(p, t)$ begins near zero for each ensemble member, the initial perturbation itself causing an imperceptible change. At each pressure level, the normalization constant k_p is set to one over twice the spatial mean, climatological variance of Z in the control integration, so that $dev_Z(p, t)$ asymptotes to 1 for large t. More important for our purposes, when it reaches 1 the control and ensemble integrations are as statistically distinct as two independent realizations of the model, and thus all memory of the initial condition has been lost.

3. Results

[8] Our ensemble forecast strategy is illustrated in Figure 1. The solid black curve in the upper panels shows the strength of the zonal mean zonal wind at 60°N and 10 hPa in the control run around the time of a major warming, with day 0 corresponding to the minimum winds. In a series of initial experiments, ensemble forecasts were launched 0, 10, 20,..., and 60 days before the warming (only 10 and 60 days are shown here). As one might expect, we find a threshold lead time, roughly 20 days for our choice of initial perturbation, which can be viewed as an uncertainty in the initial conditions, beyond which the SSW ceases to be predictable: contrast the scatter of the green trajectories from an ensemble launched 60 days before the event (1a) to the red trajectories launched 10 days before the event (1b). We find that the stratosphere behaves qualita-
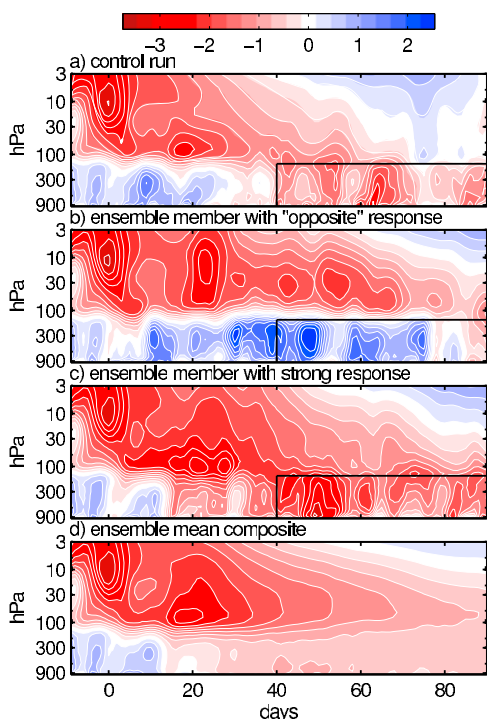
Figure 2. The NAM index as a function of pressure and time for (a) the control integration, (b) an ensemble member with seemingly no tropospheric response, (c) an ensemble member with a strong downward signal, and (d) the ensemble mean composite, averaged for 100 integrations. The plots are based on event 1, the forecast experiment illustrated in Figures 1b and 1d, and day 0 marks the SSW onset. The sign of the tropospheric response listed in Table 1 is determined from the NAM index in the black boxes in the lower right corners.

tively different after a warming, with less spread in the trajectories that share a common warming event, as found by *Mukougawa et al.* [2009] with an operational forecast model. The decreased spread of the ensemble reveals an opportunity for extended predictability. As argued by *Gerber and Polvani* [2009], the slow thermal relaxation time scales of the lower stratosphere in part explain the slow recovery of the vortex. In addition, however, the weak winds above the tropopause limit the propagation of planetary wave activity from the troposphere, cutting off the dominant source of stratospheric variability.

[9] In contrast, the overall predictability of the troposphere is not sensitive to the presence or absence of a warming event. Figures 1c and 1d show the normalized mean square deviation of geopotential height dev_Z at 500 hPa. Quantitatively similar plots are found in other tropospheric variables, e.g., surface pressure, geopotential height, and eddy kinetic energy, at all levels below the tropopause. The perturbation variance initially grows exponentially, approximately doubling every two days. Nonlinear effects become important after one week, and the variance saturates after approximately three weeks. In all cases, we find that the tropospheric circulations of the ensemble members are effectively independent after

30 days. At this time, dev_Z has reached unity, indicating that the perturbation ''anomalies'' are as large as the circulation itself and any memory of the initial condition has been expunged from the flow.

[10] Figure 1 reveals a key separation in time scales between the troposphere and stratosphere. Synoptic scale dynamics rapidly erase the initial condition in the troposphere [e.g., *Lorenz*, 1963]. Divergence of the tropospheric circulation then propagates upward into the stratosphere, in general leading to a loss of predictability after approximately one month – the longer time scale set by slower decorrelation of the planetary waves in the troposphere, as compared to the synoptic scale waves. After a major SSW, however, the stratospheric circulation remains more predictable. We exploit this separation in time scales to couple multiple realizations of the troposphere to the same stratospheric warming, essentially allowing us to build *Baldwin and Dunkerton*'s [2001] composite using a single event: 100 member ensembles are launched 10 days before 4 major warming events selected from the control integration. The 10 day lead period ensures that all ensemble members experience the warming, but also allows the tropospheric circulation time to diverge before the stratosphere recovers.

[11] We first focus on the impact of tropospheric internal variability on stratosphere-troposphere coupling. Figure 2a shows the NAM index as a function of height and lag in the control run for the event illustrated in Figures 1b and 1d. For this event, the troposphere is initially in a positive NAM state, and the stratospheric signal appears to propagate downward approximately one month after the warming. Figure 2b, however, illustrates an ensemble member where the same stratospheric event appears unable to penetrate the troposphere; if anything, the stratosphere in this integration experiences a stronger, more persistent warming, but the troposphere fails to respond. Figure 2c shows the other extreme, an integration with a seemingly powerful response in the troposphere. The key difference between the ensemble members is the internal variability of the troposphere. Only by averaging over all ensemble members (Figure 2d) can we see the ''deterministic'' response to the stratospheric perturbation, a weak but significant response at long lags. On average, it appears that the signal from the stratosphere penetrates to the troposphere after 10 days, as suggested by *Baldwin and Dunkerton* [2001], but here we focus on the long term response, past 40 days, after which time all memory of the initial condition has been erased in the troposphere. At these later times, one can be confident that the signal in the troposphere must have been mediated by the stratosphere.

[12] To quantify the variation across the entire ensemble, we focus on the tropospheric NAM response averaged over days 40 through 90 in each ensemble member, as illustrated by the boxes in Figure 2. The first row of Table 1 shows the breakdown for the event shown in Figure 2: in 88 of 100 ensemble members, the NAM is negative over this period (as in Figures 2a and 2c) and only 12 times do we see a positive NAM (as in Figure 2b). The probability of finding a negative average NAM in 88 or more of 100 randomly selected 50 day periods in the control integration is approximately 3e-14, as shown in the last column of Table 1. Ensembles were launched around three other SSW events in the control run, and the results are shown lower in Table 1.

Table 1. Tropospheric NAM Response in the Ensemble SSW Forecasts[a]

Event	Initial State	Negative	Positive	Ratio	Probability
1	positive	88	12	7.3	3.1e-14
2	positive	71	29	2.4	1.1e-4
3	negative	78	22	3.5	1.0e-7
4	negative	59	41	1.4	0.11

[a]Column 2 lists the tropospheric NAM state at the SSW onset, columns 3 and 4: the number of instances the tropospheric NAM is negative or positive, averaged over the last 50 days of the integration (40–90 days after the SSW event), and column 5: the ratio between them. The probabilities in column 6 show the chances of randomly obtaining a distribution this biased (or more so) in 100 randomly chosen 50 day intervals from the control run.

We find that in all cases a negative response dominates the ensemble. The NAM as a function of height and lag for the control run and the ensemble mean composite of these other events are illustrated in Figure 3.

[13] Figure 3 indicates that the variability in the tropospheric response depends both on the depth of the stratospheric warming, and the initial conditions of the troposphere. Events 1 (Figure 2a) and 3 (Figure 3c) are both deep warmings. Here the signal penetrates to the troposphere regardless of the tropospheric initial conditions. Events 2 and 4 (Figures 3a and 3e) were chosen because the initial warming (at day 0), did not penetrate as deeply in the control run. In these cases, the signal in the troposphere is weaker, especially in event 4.

[14] Figures 2d, 3b, 3d, and 3f show composites for a single event similar to those in the work by *Baldwin and Dunkerton* [2001]. Downward propagation from stratosphere to troposphere appears only in events in which the tropospheric NAM is initially neutral or positive; otherwise the response appears synchronous, as in Figures 3d and 3f. As SSWs occur independently of the initial state of the tropospheric NAM, half the time the troposphere will be in the positive NAM state. In these cases, it takes on the order of 10–20 days, the e-folding timescale of the tropospheric NAM, for the troposphere to adjust to the stratospheric

perturbation, producing the delay observed by *Baldwin and Dunkerton* [2001].

4. Discussion and Conclusions

[15] We have demonstrated with a relatively simple model that the persistent equatorward shift of the tropospheric jet stream following a Stratospheric Sudden Warming is mediated through the stratosphere. The slow recovery of the polar vortex in the lowermost stratosphere following an SSW provides an additional source of memory for the troposphere, leading to the persistent equatorward shift of the eddy driven jet. Thus, even though the SSW is initially forced by wave activity from the troposphere [*Polvani and Waugh*, 2004], the signal from the event is preserved in the stratosphere and is then able to influence the troposphere at long lags. As seen from differences between the ensembles members, internal tropospheric variability is large compared to the stratospheric influence, often masking the stratospheric signal. The stratospheric influence can only be seen in composites of multiple events [e.g., *Baldwin and Dunkerton*, 2001], or in ensemble composites around a single event, as shown here.

[16] Our experiments also suggest conditional limits to the predictability gain from the stratosphere. As SSWs are driven by wave activity from the troposphere, their predictably is limited by the chaotic nature of the troposphere. Once a warming has occurred, however, there is hope for a mild increase in predictability on the long time scales of the lower stratosphere. Furthermore, not all SSW events are created equal; a sharp reversal of the zonal winds at 10 hPa does not guarantee deep penetration through the stratosphere, and it is the lower stratosphere that appears to influence the troposphere.

[17] The ability of our idealized model to capture stratosphere-troposphere coupling suggests that the mechanism(s) behind the coupling lie in the large scale atmospheric dynamics. Two primary pathways for stratospheric influence have been identified: a direct, balanced response to the
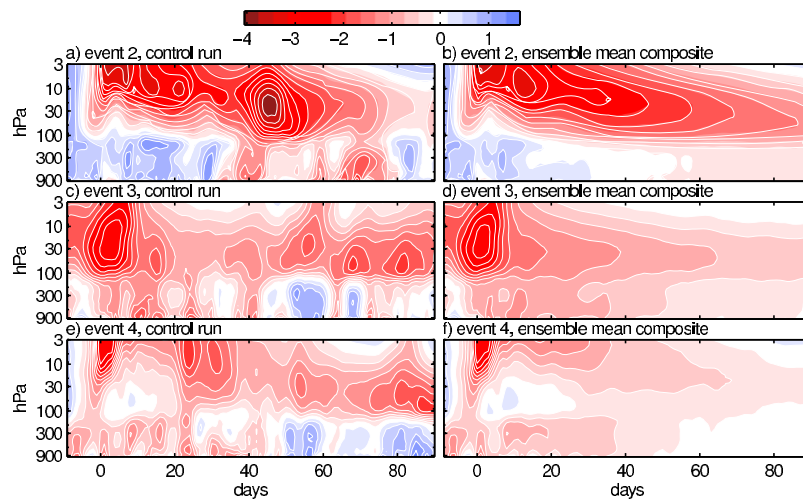

Figure 3. The NAM index as a function of pressure and time in the (a, c, and e) control integration and (b, d, and f) ensemble mean composite for SSW events 2, 3, and 4. These plots are to be compared with those in Figures 2a and 2d, for event 1.

stratospheric potential vorticity anomaly [e.g., *Hartley et al.*, 1998; *Thompson et al.*, 2006], or influence of the lower stratospheric winds on tropospheric eddies [e.g., *Wittman et al.*, 2004; *Song and Robinson*, 2004; *Chen and Zurita-Gotor*, 2008]. While our experiments cannot distinguish between these mechanisms, we have cemented the role of the stratosphere in the tropospheric response to SSWs, despite the fact that initial signal is forced from below, as noted by *Plumb and Semeniuk* [2003]. Our results thus suggest the value of resolving the stratosphere and assimilating stratospheric data in forecast models.

References

Baldwin, M. P., and T. J. Dunkerton (2001), Stratospheric harbingers of anomalous weather regimes, *Science*, *294*, 581–584.

Baldwin, M. P., D. B. Stephenson, D. W. J. Thompson, T. J. Dunkerton, A. J. Charlton, and A. O'Neill (2003), Stratospheric memory and skill of extended-range weather forecasts, *Science*, *301*, 636–640.

Boville, B. A. (1984), The influence of the polar night jet on the tropospheric circulation in a GCM, *J. Atmos. Sci.*, *41*, 1132–1142.

Charlton, A. J., A. O'Neill, W. A. Lahoz, and A. C. Massacand (2004), Sensitivity of tropospheric forecasts to stratospheric initial conditions, *Q. J. R. Meteorol. Soc.*, *130*, 1771–1792.

Chen, G., and P. Zurita-Gotor (2008), The tropospheric jet response to prescribed zonal forcing in an idealized atmospheric model, *J. Atmos. Sci.*, *65*, 2254–2271.

Gerber, E. P., and L. M. Polvani (2009), Stratosphere-troposphere coupling in a relatively simple AGCM: The importance of stratospheric variability, *J. Clim.*, *22*, 1920–1933.

Hartley, D. E., J. T. Villarin, R. X. Black, and C. A. Davis (1998), A new perspectiv on the dynamical link between the stratosphere and troposphere, *Nature*, *391*, 471–474.

Kuroda, Y. (2008), Role of the stratosphere on the predictability of medium-range weather forecast: A case study of winter 2003–2004, *Geophys. Res. Lett.*, *35*, L19701, doi:10.1029/2008GL034902.

Lorenz, E. N. (1963), Deterministic nonperiodic flow, *J. Atmos. Sci.*, *20*, 130–141.

Marshall, A. G., A. A. Scaife, and S. Ineson (2009), Enhanced seasonal prediction of European winter warming following volcanic eruptions, *J. Clim.*, *22*, 6168–6180.

Mukougawa, H., T. Hirooka, and Y. Kuroda (2009), Influence of stratospheric circulation on the predictability of the tropospheric Northern Annular Mode, *Geophys. Res. Lett.*, *36*, L08814, doi:10.1029/2008GL037127.

Norton, W. A. (2003), Sensitivity of Northern Hemisphere surface climate to simulation of the stratospheric polar vortex, *Geophys. Res. Lett.*, *30*(12), 1627, doi:10.1029/2003GL016958.

Plumb, R. A., and K. Semeniuk (2003), Downward migration of extratropical zonal wind anomalies, *J. Geophys. Res.*, *108*(D7), 4223, doi:10.1029/2002JD002773.

Polvani, L. M., and P. J. Kushner (2002), Tropospheric response to stratospheric perturbations in a relatively simple general circulation model, *Geophys. Res. Lett.*, *29*(7), 1114, doi:10.1029/2001GL014284.

Polvani, L. M., and D. W. Waugh (2004), Upward wave activity flux as a precursor to extreme stratospheric events and subsequent anomalous surface weather regimes, *J. Clim.*, *17*, 3548–3554.

Scaife, A. A., J. R. Knight, G. K. Vallis, and C. K. Folland (2005), A stratospheric influence on the winter NAO and North Atlantic surface climate, *Geophys. Res. Lett.*, *32*, L18715, doi:10.1029/2005GL023226.

Song, Y., and W. A. Robinson (2004), Dynamical mechanisms for stratospheric influences on the troposphere, *J. Atmos. Sci.*, *61*, 1711–1725.

Thompson, D. W. J., J. C. Furtado, and T. G. Shepherd (2006), On the tropospheric response to anomalous stratospheric wave drag and radiative heating, *J. Atmos. Sci.*, *63*, 2616–2629.

Wittman, M. A. H., L. M. Polvani, R. K. Scott, and A. J. Charlton (2004), Stratospheric influence on baroclinic lifecycles and its connection to the Arctic Oscillation, *Geophys. Res. Lett.*, *31*, L16113, doi:10.1029/2004GL020503.

———————

E. P. Gerber, Center for Atmosphere Ocean Science, Courant Institute of Mathematical Sciences, New York University, 251 Mercer St., New York, NY 10012, USA. (gerber@cims.nyu.edu)

C. Orbe and L. M. Polvani, Department of Applied Physics and Applied Mathematics, Columbia University, 200 S.W. Mudd Bldg., MC 4701, 500 W. 120th St., New York, NY 10027, USA.